

# MEASUREMENTS OF T-S WAVES DUE TO ACOUSTIC DISTURBANCES IN EXPERIMENTS

Zhen Cao<sup>1</sup>, Peifan Li<sup>2</sup> & Dong Li<sup>3</sup>

<sup>1</sup>School of Aeronautics, Northwestern Polytechnical University, Xi'an 710072, China

#### **Abstract**

Boundary-layer receptivity to external disturbances plays a key role in transition from laminar to turbulent flow. However, studying the process of how disturbances become entrained in the boundary layer remains challenging, especially in experiments. As a common external disturbance, the acoustic disturbance interacts with the localized roughness to create Tollmien–Schlichting (T-S) waves in the boundary layer. Measurements of T-S waves under this situation is complicated mainly by the presence of the Stokes wave which has the same frequency with the former. This study isolated the T-S waves from the Stokes waves in two varied ways under both continuous and pulsed acoustic disturbances and compare their results with the linear stability theory (LST). The receptivity to acoustic disturbances with different thickness of the 2-D roughness was also evaluated quantitatively, which is consistent with other numerical results.

**Keywords:** Boundary layer Receptivity T-S wave Flow control

#### 1. Introduction

The laminar–turbulent transition process has been a research hotspot for several decades, for an understanding of it is crucial for design and optimization in aerodynamic applications. However, there are still some stages not yet fully understood, especially in experimental studies. As the first stage of the transition, receptivity[1] decides the initial amplitude of the perturbations and the way to develop to the next stage, which can be used to forecast the location of the transition. For a given flow, external disturbances are introduced into the boundary layer, then after the receptivity stage, the instability waves are generated and developed. Transition often occurs when the amplitude of the instability waves reaches a certain critical level.

In this paper, the response of the boundary layer on a finite-thickness flat plate with a local roughness tape on the surface of it to acoustic waves were investigated. Acoustic disturbances enter the boundary layer, combined with the local roughness tape to excite a variety of unsteady modes. When the amplitude of the acoustic waves and the scale of the roughness tape are in a certain range, the unsteady modes can be the Stokes (plane acoustic waves) and Tollmien—Schlichting (T-S) waves. Measurements of the T-S waves under this situation are difficult due to the presence of Stokes waves which has the same frequency as the T-S waves.

Saric *et. al* [2] studied this problem experimentally in 1995 and summarized two universal methods to extract T-S waves. One method is suitable for the situation under which the disturbance is continuous, which was earlier employed by Wlezien[3]. Since the T-S wavelength is two orders of magnitude shorter than the acoustic wavelength, a streamwise scan that covers one T-S wavelength at a constant height from the flat plate, is nearly one of constant phase for the Stokes wave. Then the amplitude and phase of the velocity fluctuation signal are plot in a polar complex plane as a spiral. The radius of the spiral represents the T-S amplitude. As this method needed a large amount of measurements, it was seldom used later.

The other method to measure the receptivity was called 'the pulsed-sound technique'. From linear stability theory, the T-S wave propagates at approximately one third the freestream speed. Therefore, the speed of a T-S wave generated by an acoustic wave is two orders of magnitude smaller than the

stokes wave. Based on this fact, the traveling T-S wave can be isolated from the Stokes wave by sending short bursts of sound into the test section. The sound burst is first measured then the T-S wave is measured after several microseconds.

Recent years, some other new methods to isolate T-S waves were proposed. A way to separate T-S waves was proposed by Monschke *et. al* [4] using the biorthogonal properties of a modified Orr-Sommerfeld equation. In 2020, a device was designed to fix the phase between situations with and without the roughness by Placidi *et. al* [5] for the studies on the localized receptivity. These two methods have not been widely used yet.

This problem has also been studied numerically [6,7]. Shahriari *et. al* [8] calculated the leading-edge receptivity of the flat plate and gave a summary on the published results. They concluded that their receptivity predictions are accurate and one order of magnitude smaller than the existing values in the literature, which is significant.

In this paper, the localized receptivity of the flat plate was investigated with both continuous and pulsed acoustic disturbances included and their measurements were under the same conditions. The results were verified and compared with the linear stability theory and past numerical results.

# 2. Experimental Methods and Settings

# 2.1 Wind tunnel and model

Experiments were presented in a low-speed wind tunnel of open-return type. The tunnel test section measured  $\phi$ 1.5m×1.9m and was equipped with a sound-proof chamber. The intensity of the flow turbulence A highly polished 1.5m long flat plate, with a span of 600mm, and a thickness of 10mm was mounted vertically in the test section. A zero-pressure gradient was achieved along the plate by varying the flat plate angle of attack. The flat plate has a modified super-ellipse (MSE) leading edge with an aspect ratio of 20:1. These shapes were used by Lin *et al.* [9] in a DNS of the receptivity problem. The geometry is described by:

$$\left(\frac{y}{b}\right)^2 + \left(\frac{a-x}{a}\right)^m = 1, m = 2 + \left(\frac{x}{a}\right)^2 \tag{1}$$

Where a is the major axis, b is the minor axis, and the coordinate origin is at the stagnation line. This shape eliminates the curvature discontinuity at the ellipse/flat-plate juncture.

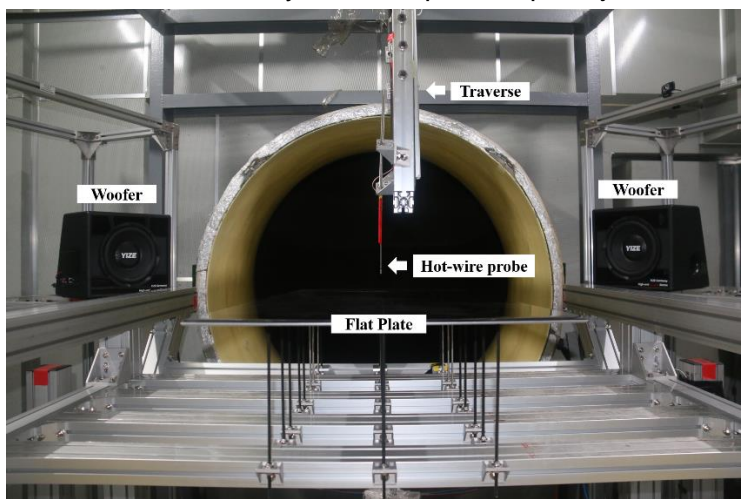


Figure 1 – Wind tunnel set-up (side view, against the flow direction).

The flat plat was installed horizontally in the wind tunnel. Figure 1 shows all set-up (the location of the woofers and the traverse, the way of the model installation, etc.) in the test section.

## 2.2 Disturbances introducing system

The acoustic disturbances were introduced by two woofers of 250 mm diameter located symmetrically at the two sides of the inlet to send acoustic disturbance into the test section, as shown in figure 1.

After amplified by the signal amplifier, acoustic disturbances were sent to the test section through

the woofers. The oscilloscope was used to monitor the signals generated. Related equipment was shown in figure 2(a). The sound pressure level in the test section is 46 dB without the disturbances and is limited to 95 dB with disturbances to avoid excessive forcing[10]. Figure 2(b) shows how the decibel meter measures the sound pressure level in the test section.



Figure 2 – The generating and measuring facilities of the acoustic disturbance.

Two kinds of acoustic disturbances in the present experiment were considered: the continuous disturbance and the pulses. Both of them are based on the sinusoidal signal and generated by the signal generator. The physical frequency *f* was chosen at a given speed.

Figure 3 shows the waveforms of the two disturbances collected by the microphones installed at the leading-edge of the flat plate.

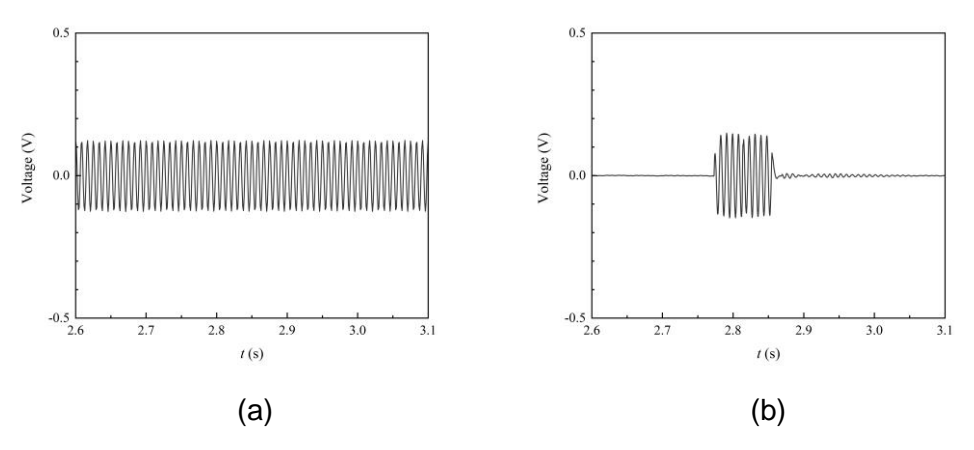


Figure 3 – The waveforms of (a) the continuous waves; (b) the pulses.

## 2.3 Measurements

Velocity measurements were obtained by a constant-temperature hot-wire anemometer (Dantec) using a 55P15 hot-wire probe. The sampling frequency was kept fixed at 9 kHz throughout the tests and lowpass and high-pass filters were applied at 2000 kHz and 30 Hz, respectively. A 3-axis traverse system was installed to move the hot-wire at streamwise, wall-normal, and spanwise directions indicated with (x, y, z), respectively.

Table 1 – Summary of test cases, measuring stations and other relative parameters
---

Case	Perturbation	f	H	L	$U_{\infty}$	Stations <i>x</i>	SPL
	type	(Hz)	(µm)	(mm)	(m/s)	(mm)	(dB)
1	Continuous	80	50	200	10	400,550,650,700	85
2	Continuous	80	180	200	10	400,550,650,700	85
3	Pulsed	80	50	200	10	400,550,650,700	95
4	Pulsed	80	180	200	10	400,550,650,700	95

Continuous acoustic disturbances and pulsed acoustic disturbances were both applied combined with a two-dimensional roughness tape located on the surface of the flat plat to excite T-S waves. The best location of the tape to excite T-S waves is branch I, where the unstable mode begins to increase. Table 1 shows all relative parameters (the forcing frequency, the location and the thickness of roughness tapes, the flow velocities, measuring stations and SPL).

When the hot-wire is very close to the wall during the measurement, the heat radiation of the hot wire will be interfered by the flat plate, and the hot-wire measurement will have a velocity deviation. The suggested value given by Saric[11] is to measure from  $u/U_{\infty}$ =0.1 and use a linear interpolation to the origin for the velocity type near the wall. In the present experiment, due to the limitation of the experimental conditions, the minimum value of  $u/U_{\infty}$  is about 0.3. Figure 4 shows the hot-wire probe when it was at the lowest point and the distance from the probe to the surface is about 0.2mm.

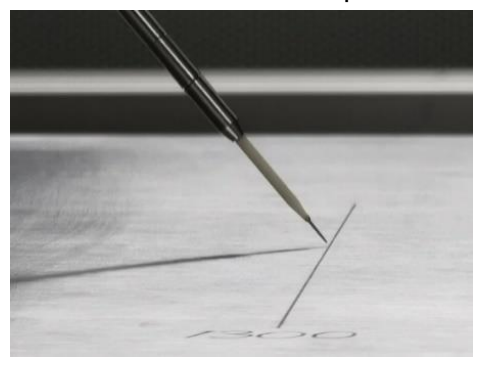


Figure 4 – The lowest location of the hot-wire probe during the measurement.

A comparison of the basic mean-velocity profiles with the theoretical Blasius profile is given in Figure 5. The velocity profiles fit well with the Blasius result, confirming the self-similarity of the profiles. At every streamwise station, situations with and without acoustic disturbances and roughness tapes were measured.

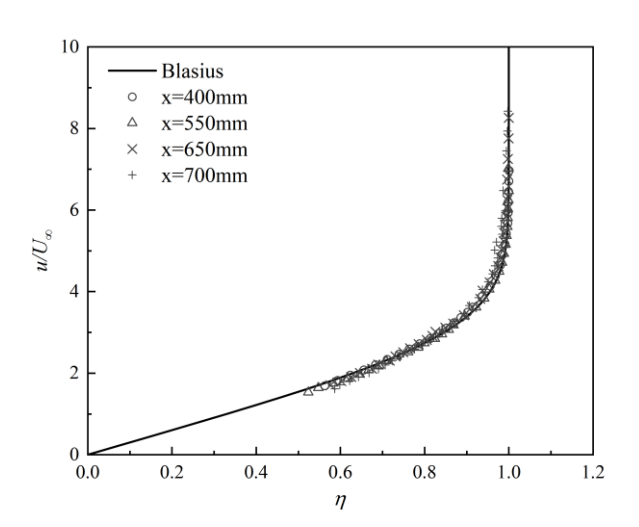


Figure 5 – Profiles of the mean streamwise velocity in the boundary layer at 5 stations ( $U_{\infty}$ =10m/s) compared with the theoretical Blasius profile.

## 2.4 The Extraction Methods of the T-S Wave

## 2.4.1 Methods for the continuous disturbance

For situations under the continuous forcing, the Fourier transform was used to acquire the amplitudes of the forcing frequency with and without the roughness tape respectively. The signal recorded by the hot-wire contains the Stokes, the T-S wave, the probe vibrations, and the electronic noise. To remove interferences, some measures of vibration damping and noise reduction were implemented. The sound-proof chamber around the test section reduced the noise from the electrical machinery of the wind tunnel. Besides, sponge strips were pasted on the bottom of the woofers to avoid the vibration. As the disturbance was continuous, the T-S wave generated was also continuous. During the measurements, their amplitudes were superposed with the same frequency. When the phase was kept, the substraction between the amplitude values with and without the roughness tape represents the amplitude of T-S waves due to the localized roughness tape employing the Fourier transform.

# 2.4.2 The pulsed sound technique

Here, the pulsed-sound forcing technique proposed by Saric et al. [2] was implemented to isolate the amplitude of the T-S waves. The pulsed-sound experiments usually introduce sound pulses (typically three- to five-cycle sine waves) to the boundary layer, and record the resulting freestream and boundary-layer hotwire signals. The boundary layer hot-wire first measures a Stokes wave and later a T-S wave passed by. The delay between the Stokes and T-S waves is due to the speed difference between them. The Stokes wave travels at sonic velocity while the T-S wave travels at a fraction of the freestream speed, which is calculated to be about one-third. Several hundred milliseconds separate the Stokes and T-S signals measured by the hot-wire. Typical velocity signals of the pulsed sound technique are shown in Figure 7. It is worthing noticing that in the present experiment, the freestream hot-wire was not installed for the limitation of the experimental conditions and the amplitude of the acoustic wave at every station was estimated by the value in the corresponding potential flow.

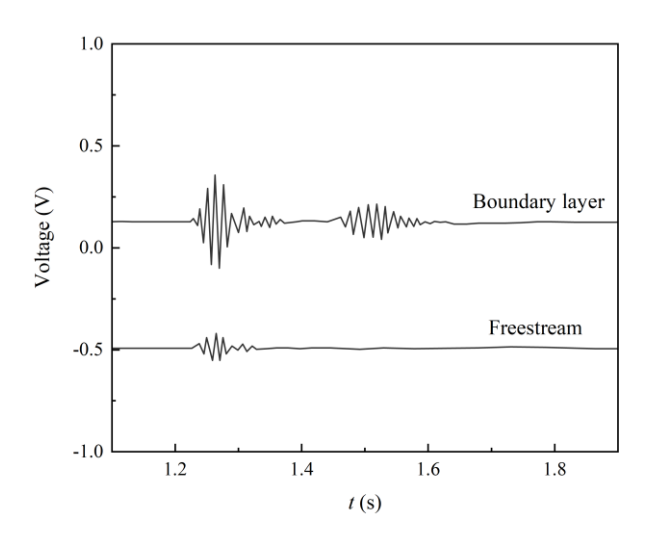


Figure 7 – Typical velocity signals of the pulsed-sound technique.

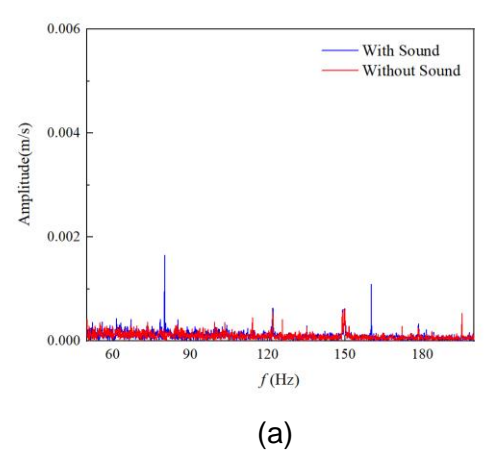
These two methods both have their advantages and disadvantages. The measurements of the situation and the data processing under the continuous disturbances are convenient, while the continuous disturbances bring a complicated environment with the reflection which cannot be eliminated completely. The pulsed-sound technique avoids the superposition of the T-S waves and the Stokes waves, however, the measurements under the pulsed-sound can be repetitive for the need of large amount of ensemble average. In the present experiment, the two methods were verified and compared with each other in the localized receptivity due the acoustic disturbance.

## 3. Results and Discussions

## 3.1 The verification of two methods

# 3.1.1 The receptivity due to the continuous forcing

Cases with and without the roughness tape were measured under the continuous acoustic forcing then the amplitude of the T-S wave was obtained by FFT. Figure 8 shows the frequency spectrum in the potential flow and the boundary layer respectively. There is no T-S wave being generated in the potential flow theoretically, so the amplitude of the signal at 80Hz represents the amplitude of the acoustic wave. While in the boundary layer, the amplitude of the signal at 80Hz represents the sum of amplitudes of the T-S wave and the acoustic wave. From figure 8, the value of the later is significantly greater than the former.



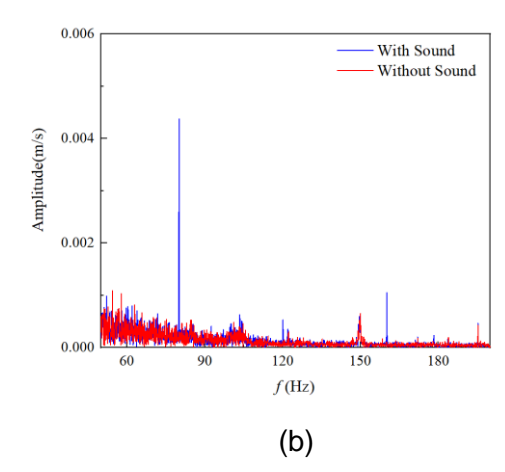


Figure 8 – Fourier transform results of the signals in (a) potential flow; (b)boundary layer. Parameters:  $U_{\infty}=10\text{m/s}$ , f=80Hz,  $h=50\text{\mu m}$ , x=650mm.

Figure 9 displays a comparison between the theoretical T-S eigenfunction mode and the T-S wave profile extracted by the current experiment for roughness heights of 50  $\mu$ m and 180 $\mu$ m at the station where x=650mm. The experimental data in figure 8 shows a distinct dual-lobe amplitude shape characteristic of T-S waves. Considering the uncertainty of the experimental conditions, discrepancies between the results of linear stability theory and experiments are acceptable, which proves the feasibility of this method.

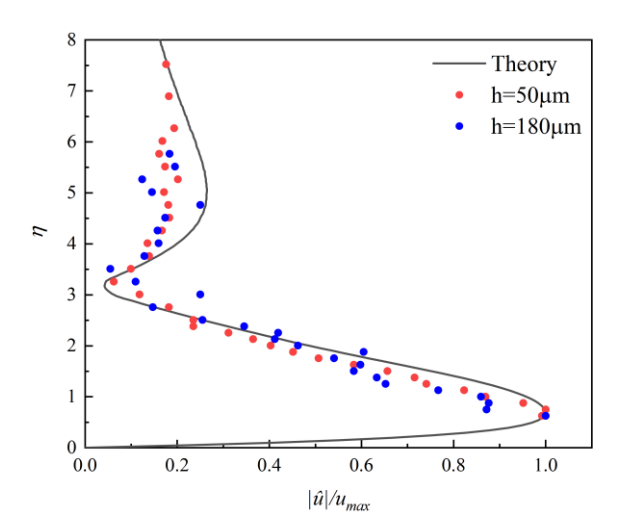


Figure 9 – Wall-normal distribution of the streamwise velocity amplitude of T-S wave at x=650mm with comparison to theoretical results: f = 80Hz,  $h_1 = 50$ µm,  $h_2 = 180$ µm.

## 3.1.2 The pulsed-sound technique

Figure 10 displays the time trace of the velocity at x=650mm, y=0.6mm with the frequency forcing f=80Hz and the roughness thickness h=180 $\mu$ m. The blue line represents the velocity in potential flow and the red line represents that in boundary layer. It is clear that there is only the acoustic wave recorded in the potential flow while the stokes wave and the T-S wave are both recorded in the boundary layer with a time delay about 0.13s, which is consistent with the theoretical value.

Similar to the situation of the continuous acoustic forcing, figure 11 displays the comparison between the theoretical T-S eigenfunction mode and the T-S wave profile under the same conditions. The experimental data in figure 11 also shows a distinct dual-lobe amplitude shape characteristic of T–S waves. Compared with figure 9, the 'second' lobe (farther from the surface of the flat-plate) in figure 11 fits better with the theoretical results.

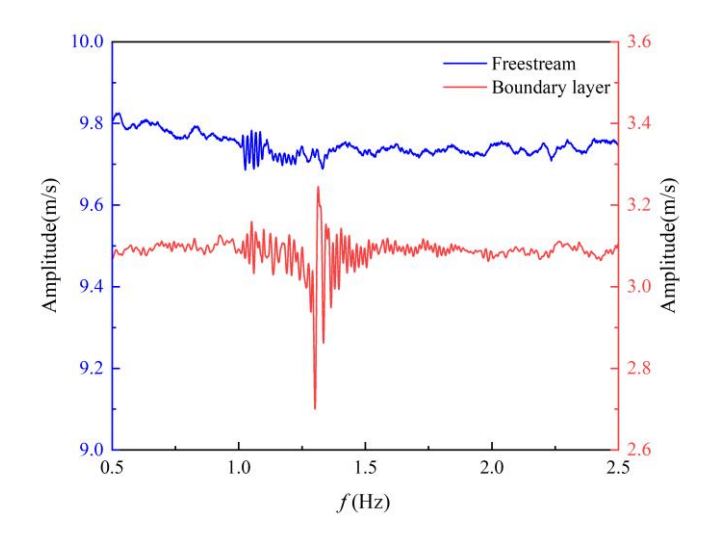


Figure 10 – Time trace of the velocity at x=650mm, y=0.6mm, f = 80Hz, h=180 $\mu$ m.

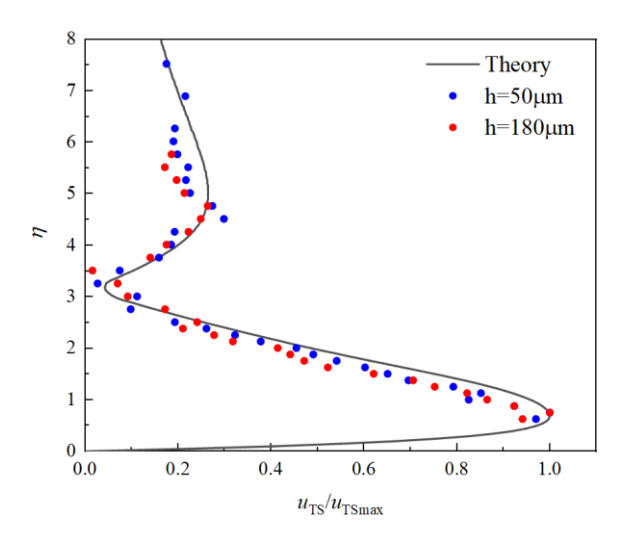


Figure 11 – Wall-normal distribution of the streamwise velocity amplitude of T-S wave at x=650mm with comparison to theoretical results: f = 80Hz,  $h_1 = 50$ µm,  $h_2 = 180$ µm.

# 3.2 The comparison of two methods

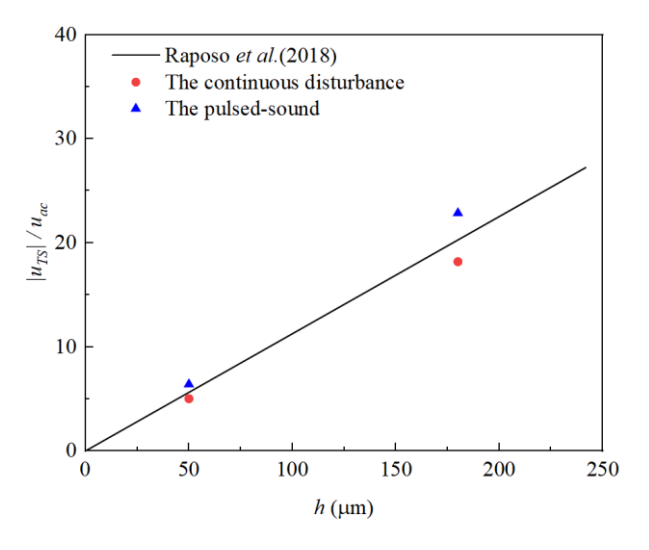


Figure 12 – Wall-normal distribution of the streamwise velocity amplitude of T-S wave at x=650mm with comparison to theoretical results: x=700mm, f=80Hz,  $h_1=50$ µm,  $h_2=180$ µm.

As the amplitudes of the T-S wave in figure 9 and 11 have been normalized by their own maximum value, they cannot be compared with each other directly. To uniform the standard with the results of Raposo *et. al* [12], the ratio of the amplitude of the T-S wave and the acoustic wave were calculated. Figure 12 shows the comparison of the results from two methods and Raposo *et. al*. Considering the uncertainty of the experimental work, the results of  $h_1$ =50µm and  $h_2$ =180µm for both methods were consistent with the numerical result of Raposo *et. al*, with the errors about 10~15%.

## 4. Conclusions

In this paper, the localized receptivity of a flat plate to two types of acoustic disturbances was studied. Their methods of the data processing to separate T-S waves and Stokes waves varied while both were credible. The T-S waves were captured by these both methods and their amplitudes were fit well with the LST results. The ratio of the amplitudes of the T-S wave and the acoustic wave for two thickness of the roughness tape ( $h_1$ =50µm and  $h_2$ =180µm) were shown and compared with the numerical results of Raposo *et. al.* The results show that the ratio under continuous acoustic disturbance were smaller than the numerical results while the ratio under pulses disturbance were greater.

# 5. Acknowledgements

The authors would like to acknowledge the support of National Natural Science Foundation of China (Grant No. 11772260).

## 6. Contact Author Email Address

Mail to: 402436085@qq.com; 2017caozhen@mail.nwpu.edu.cn

# 7. Copyright Statement

The authors confirm that they, and/or their company or organization, hold copyright on all of the original material included in this paper. The authors also confirm that they have obtained permission, from the copyright holder of any third-party material included in this paper, to publish it as part of their paper. The authors confirm that they give permission, or have obtained permission from the copyright holder of this paper, for the publication and distribution of this paper as part of the ICAS proceedings or as individual off-prints from the proceedings.

#### References

- [1] Morkovin, M. V., "On the Many Faces of Transition," Boston, MA, 1969. https://doi.org/10.1007/978-1-4899-5579-1 1
- [2] Saric, W., Wei, W., Rasmussen, B., and Krutckoff, T., "Experiments on Leading-Edge Receptivity to Sound," Fluid Dynamics Conference, American Institute of Aeronautics and Astronautics, 1995. https://doi.org/10.2514/6.1995-2253
- [3] Wlezien, R., "Measurement of Acoustic Receptivity," presented at the Fluid Dynamics Conference, Colorado Springs, CO, U.S.A., 1994. https://doi.org/10.2514/6.1994-2221
- [4] Monschke, J. A., Kuester, M. S., and White, E. B., "Acoustic Receptivity Measurements Using Modal Decomposition of a Modified Orr–Sommerfeld Equation," *AIAA Journal*, Vol. 54, No. 3, 2016, pp. 805–815. https://doi.org/10.2514/1.J054043
- [5] Placidi, M., Gaster, M., and Atkin, C. J., "Acoustic Excitation of Tollmien–Schlichting Waves Due to Localised Surface Roughness," *Journal of Fluid Mechanics*, Vol. 895, 2020, p. R5. https://doi.org/10.1017/jfm.2020.349
- [6] Fuciarelli, D., Reed, H., and Lyttle, I., "Direct Numerical Simulation of Leading-Edge Receptivity to Sound," *AIAA Journal*, Vol. 38, No. 7, 2000, pp. 1159–1165. https://doi.org/10.2514/2.1109
- [7] Wanderley, J. B. V., and Corke, T. C., "Boundary Layer Receptivity to Free-Stream Sound on Elliptic Leading Edges of Flat Plates," *JOURNAL OF FLUID MECHANICS*, Vol. 429, 2001, pp. 1–21. https://doi.org/10.1017/S0022112000002548
- [8] Shahriari, N., Bodony, D. J., Hanifi, A., and Henningson, D. S., "Acoustic Receptivity Simulations of Flow Past a Flat Plate with Elliptic Leading Edge," *JOURNAL OF FLUID MECHANICS*, Vol. 800, 2016, p. R2. https://doi.org/10.1017/jfm.2016.433
- [9] Lin, N., Reed, H. L., and Saric, W. S., "Effect of Leading-Edge Geometry on Boundary-Layer Receptivity to Freestream Sound," *Instability, Transition, and Turbulence*, edited by M. Y. Hussaini, A. Kumar, and C. L. Streett, Springer New York, New York, NY, 1992, pp. 421–440. https://doi.org/10.1007/978-1-4612-2956-8 42
- [10] Nishioka, M., and Morkovin, M. V., "Boundary-Layer Receptivity to Unsteady Pressure Gradients: Experiments and Overview," *Journal of Fluid Mechanics*, Vol. 171, No. 1, 1986, p. 219. https://doi.org/10.1017/S002211208600143X
- [11] Saric, W. S., "Experiments in 2-D Boundary Layers: Stability and Receptivity," presented at the AVT-151 RTO AVT/VKI Lecture Series, von Karman Institute, Rhode St. Genèse, Belgium, 2008.
- [12] Raposo, H., Mughal, S., and Ashworth, R., "Acoustic Receptivity and Transition Modeling of Tollmien-Schlichting Disturbances Induced by Distributed Surface Roughness," *Physics of Fluids*, Vol. 30, No. 4, 2018, p. 044105. https://doi.org/10.1063/1.5024909